

# Design and Stabilization of near concentric cavities

ChiHuan Nguyen,<sup>1</sup> Adrian Nugraha Utama,<sup>1</sup> Nick Lewty,<sup>1</sup> and Christian Kurtsiefer<sup>1,2</sup>

<sup>1</sup>*Centre for Quantum Technologies, 3 Science Drive 2, Singapore 117543*

<sup>2</sup>*Department of Physics, National University of Singapore, 2 Science Drive 3, Singapore 117542\**

(Dated: March 30, 2018)

We report on the compact design, construction and stabilization of a Fabry-Perot near-concentric cavity with a length of 11mm. The cavity is designed to obtain strong coupling regime of cavity quantum electrodynamics (CQED) with single neutral atoms, and with large physical space, can be extended to include ions or other collective quantum emitters. We demonstrate the long term stability of the cavity operated at an optical cavity length of sub-wavelength shorter than the concentric point, which corresponds to the stability parameter  $g = -0.999996(28)$ .

PACS numbers: 32.90.+a, 37.30.+i, 42.50.Ct

## I. Introduction.

Optical cavities are indispensably used in modern technologies ranging from lasers, gravitational wave detectors, and applications of quantum technologies which require nonlinear atom-light interaction. In particular, atoms-cavity systems with ultra-high finesse cavities have been widely used by several groups to demonstrate quantum logic gates, quantum distributed networks, quantum metrology and quantum sensing [1-3]. Though displaying remarkable achievements, the intricate high-reflectivity coating of the cavity mirrors used in these experiments poses a challenge on scaling up the system. As a result, there is an increasing trend of exploring new types of optical cavities which can provide additional advantages [4, 5]. Recently, one of such proposed cavity designs that has been experimentally demonstrated is near-concentric Fabry-Perot cavities [5]. Outside of the atomic physics community, there are also reports and suggestions of using near-unstable cavities (NUC) such as concentric cavities to reduce mirror coating thermal noise [6].

Among all geometrical configurations of Fabry-Perot cavities, concentric cavities, where the length of the cavity is twice the radius of curvature of cavity mirrors:  $l_{cav} = 2R_C$ , exhibits the tightest focusing mode at the waist of the cavity. This strong focusing mode, which in ideal conditions can reach diffraction-limited waist, effectively concentrates the cavity field at the location of the trapped atoms. Therefore, despite being operated at millimeter cavity length, the near-concentric cavity can provide a substantially small effective mode volume comparable to the state-of-the-art microcavities. The millimeter cavity length allows one to obtain narrow cavity linewidth with relative low finesse mirrors, more optical access and space to prepare and manipulate quantum matters inside the cavity. Furthermore, the near-degeneracy in resonant frequencies of transverse modes of near-concentric cavities is also an intriguing feature to explore the physics of multi-mode strong coupling cavity

quantum electrodynamics [7].

Despite these advantages, near-concentric cavities have not been widely explored yet mainly because of technical hurdles of constructing and stabilizing them. It is due to the fact that the concentric cavity is close to the margin of the stability curve and hence sensitive to the misalignment in the transverse positions of the two cavity mirrors. Though shortly mentioned in some textbooks, to the extent of our knowledge, there has not been a report or any technical account to describe the construction and stabilization of concentric cavities.

Here, we report a compact design of a 11mm length near-concentric cavity stabilized at subwavelength shorter than concentric point. In addition, we demonstrate the long-term stability of the cavity. The design is particularly used to study trapped atoms-light interaction but can be easily adapted to a wider range of other experiments. The paper is organized as follows. In Section I, the cavity design is described and followed by the alignment procedure in Section II. In Section III, we discuss about the transverse modes spacing measurement to characterize how far the cavity is away from the concentric point. We also address the issue of cavity stabilization in transverse directions in Section IV.

## II. Cavity system design

### 1. Design of cavity mirrors

We first describe the design of our cavity system. Central to our system is the spherical cavity mirrors with the radius of curvature  $R_C = 5.5$  mm, and nominal reflectivity of  $R = 99.5\%$  at wavelength of 780 nm. To have an effective mode-matching, the input surface of the mirror has an aspherical shape instead of an usual planar surface, which is introduced to transform the collimated gaussian beam into the desired cavity mode. The details of characterization and aberration analysis of the mirrors can be found somewhere else [8].

### 2. Piezo

Close to concentric length, the cavity alignment is sensitive to transverse directions. In order to be able to align the cavity and correct for misalignment due to thermal drifting, we placed one of the cavity mirrors on a stacked piezo (PI P-153.10H). The piezo consists of 72 stacks glued together, which can be grouped into three segments

---

\* christian.kurtsiefer@gmail.com

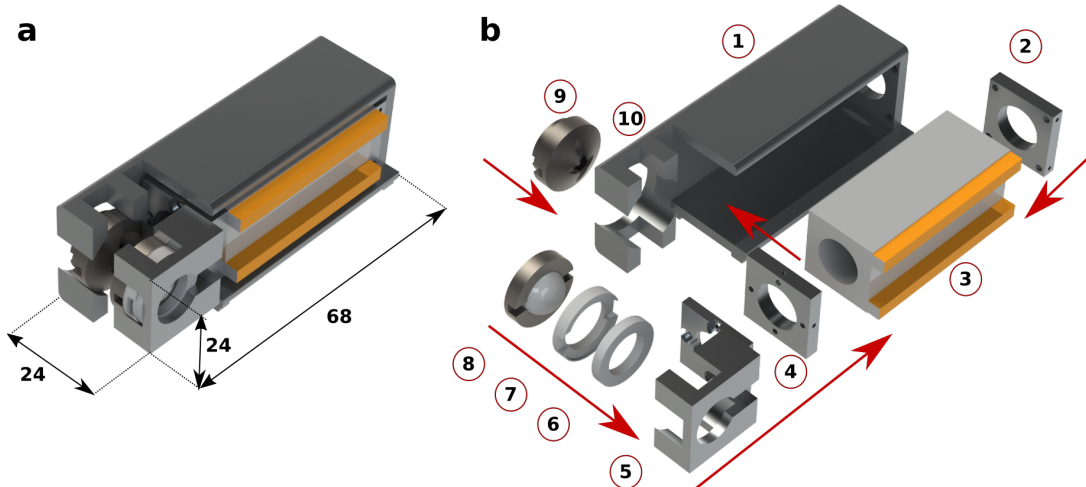


FIG. 1. Three-dimensional model of the near-concentric cavity system. (a) The completed assembly view with system dimensions in millimeters. (b) The exploded view: 1 The cavity holder. 2 The back plate. 3 The stacked piezo. 4 The front plate. 5 The L-shaped block. 6 The disc piezo. 7 The PEEK spacer. 8 The right cavity mirror in the shield. 9 The left cavity mirror in the shield. 10 The spherical opening. The yellow bars indicate the piezo electrodes. Arrows show the direction of assembling parts.

corresponding to three orthogonal travelling directions. In each direction, the piezo is able to move  $\pm 5\mu\text{m}$  with sub-nanometer resolution. In addition, there is another ring piezo which can cover a shorter travelling distance but provides a higher locking bandwidth.

### 3. Cavity mounting system

The cavity mounting system is designed to be compact and fit to a scientific cuvette which can provide excellent optical access to the experiment. Fig. 1 shows the schematics of our design. The system essentially consists of the following parts: a piezo holder, cavity mirror shields, and a L-shaped block. Except the cavity mirror shields, all the mechanical parts are made from Titanium to reduce the structural change of the mounting system due to thermal fluctuation.

The cavity mirror is placed into an aluminum cavity mirror shield and secured with a vacuum-compatible epoxy. The shields provide general protection and prevent the cavity mirrors from being contaminated by sputtered atomic beam used in atom trapping experiments. The piezo holder is the main body of the cavity mounting system and used to accommodate the stack piezo. The holder is machined on a computer numerical controlled (CNC) milling machine from a block of Ti6Al4V Grade-5 titanium. The piezo holder has a protruding arm with a spherical opening to hold one of the cavity mirrors. The four columns at the opening provide anchor points to glue the cavity mirror. The other mirror would be mounted inside a similar structure located on the L-shaped block. The diameter of the spherical openings is  $\sim 100\mu\text{m}$  larger than the diameter of the mirror shields. The gap between the shield and the four columns allows adjustment of the mirror's position during the alignment process. Larger size of the gap, though allows for more

tolerance in the machining process, requires more glues to apply and hence causes more drifting of cavity mirrors' position during the curing process.

### II. Alignment Procedure

We proceed to describe the cavity mirror alignment procedure. Contrary to other cavity configurations, the relative transverse positions of the two mirrors of the concentric cavity is critical. The requirement for the transverse alignment is that the two optical axes of the mirrors must be coincident. Here we list out the steps required to align the two cavity mirrors and assemble them into the mounting system. Fig. 2 shows the schematics of our alignment setup. The first step is to have an optical setup of two fiber-couplers coupled to each other. The laser beam between two fiber-couplers defines a reference line for the alignment of the cavity mirrors. In other words, the optical axis of two cavity mirrors will be aligned to be coincident with the reference laser beam. This provides a coarse alignment of cavity and finer adjustment will be done later by maximizing the transmission of the fundamental mode of the cavity. The cavity mounting system with one glued cavity mirror is stationed on a xyz precision translation stage (Thorlabs PT3/M) with a tip-tilt mirror mount (KM100-E02). This arrangement allows adjustment of full degrees of freedom in translation and two rotational degrees of freedom. The next step is to align the translation stage such that the laser beam hit the center of the cavity mirror. This can be ensured by observing the symmetry of the reflected beam from the mirror on a camera. The adjustment of the tip-tilt mirror is used to make the reflected beam from the cavity mirror back to the fiber coupler. On the left side, the other mirror (that we call left mirror) is clamped to a delivery holder, which is moved around by a transla-

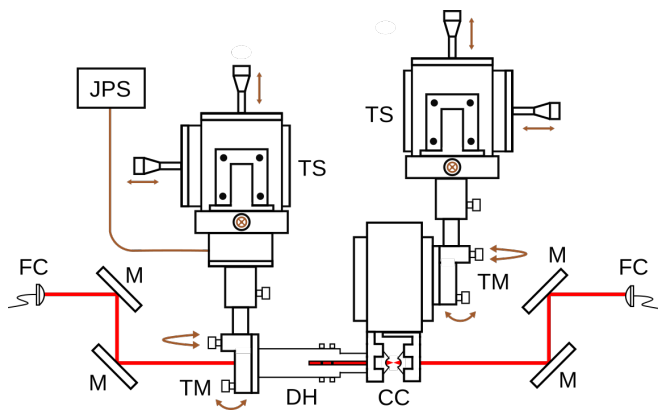


FIG. 2. Schematic of cavity alignment setup. Two single-mode fiber couplers (FC) coupled to each other define a reference line for the optical axis of concentric cavity (CC). Delivery holders (DH) is placed on the left translation stage with a Jena Piezo System (JPS). The cavity mounting system is on the right translation stage (TS). Rotational degrees of freedom are provided by tip-tilt mounts (TM). M: highly reflective mirrors.

tion stage. The mirror can be released from the holder by untightening the screws on the top of the delivery holder after the gluing process. Following the same procedure, the left mirror optical axis is aligned along the reference beam. Here, beside the coarse movement of the micrometer knob, the left mirror can be moved with nm resolution step provided by the Jena piezo system (part number). When the two cavity mirrors are well aligned with the reference beam, the left mirror is slowly moved into the holder through the spherical opening of the cavity holder. In order for the left mirror to avoid touching the cavity holder which can alter the alignment, we monitor the electrical continuity between the two holders with a multimeter. In addition, the optical power of the reflected beam into the fiber couplers was made sure to be relatively constant during the transport process. When the cavity mirror is totally inside the holder, fine adjustment of the transverse position is done with the Jena piezo system. The transmission of the cavity detected on photodiode is used as a feedback for the alignment. Note that during the alignment procedure, the alignment of laser beams are maintained fixed, only the positions of two cavity mirrors are adjusted to get the optimized cavity transmission.

When the alignment is done, vacuum-compatible epoxy (Torrseal) are applied at the contacts between the cavity mirror shield and the four columns at the spherical opening of the holder. Torrseal is chosen because of its relatively low shrinkage, ultrahigh vacuum compatibility and high elasticity modulus. We observe that the curing process can change volume of glues and hence pushing the cavity mirror out of the alignment, so it is critical to apply an equal amount of glues at the four corners to balance the drifting during the curing process. We observe that it takes about two hours at room temperature

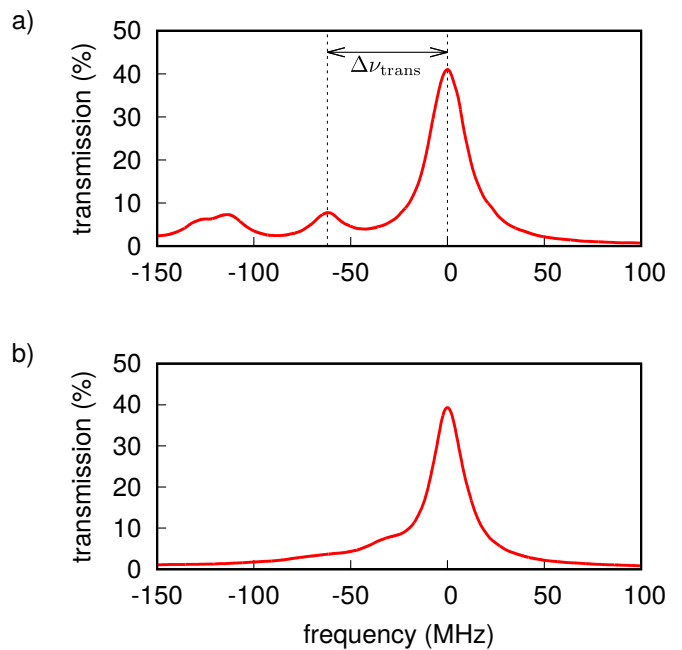


FIG. 3. Cavity transmission spectra for multiple cavity lengths. (a)  $L = 2R - 600$  nm. Vertical dashed lines indicate the resonant frequencies of  $TEM_{00}$  and  $TEM_{01}$  (b)  $L = 2R - 210$  nm. High-order transverse modes become degenerate and form a long tail extending out to lower frequencies.

for the Torrseal to be cured and hardened. During the curing process, the cavity mirrors position needs to be constantly monitored and adjusted to maintain the cavity alignment. After the mirror's position is secured by the cured Torrseal, the mirror is released from the delivery holder and the holder is withdrawn out, leaving the cavity mirrors assembled and aligned inside the cavity holder.

### III. Transverse Mode Spacing Measurement

Laguerre-Gaussian (LG) functions form a complete basis to solutions of the paraxial wave equation, and thus can be used to describe the eigenmodes of spherical optical resonator. We denote cavity modes as  $LG_{nlp}$  where  $n, l, p$  are integer numbers. Modes of different  $n$  are known as the longitudinal modes, while the indices  $(l, p)$  indicate spatial dependences of the cavity modes on transverse coordinates, hence known as transverse modes. The resonance frequencies of the cavity modes are determined by the condition that the round-trip phase shift in the cavity must be an integer multiple of  $2\pi$ . As the cavity length approaches concentric point, the shift of the transverse modes frequency approaches the free spectral range; therefore all transverse modes become co-resonant in the concentric regime.

Making use of this property, we determine cavity length by measuring the difference of resonance frequencies between the fundamental mode  $LG_{00}$  and the transverse mode  $LG_{10}$ . Under paraxial approximation, the resonance frequencies of the cavity with identical spher-

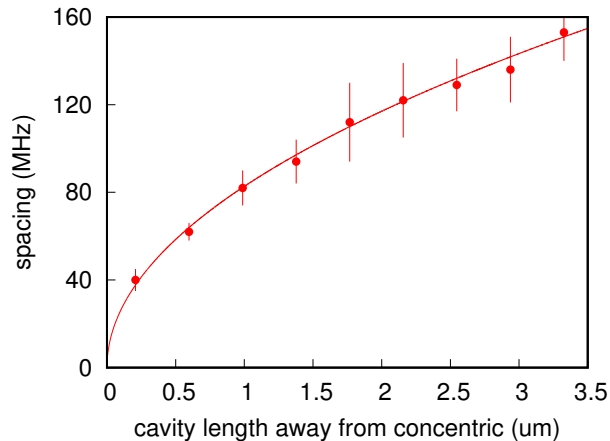


FIG. 4. Transverse mode frequency spacing at different cavity lengths that are resonant with 780 nm laser. Solid line are theoretical fit based on Eq. 2. Error bars show the standard deviation of the measurement.

ical mirrors are given by:

$$\nu_{n,l,p} = n \frac{c}{2l_{cav}} + (1 + |l| + 2p) \frac{c}{2l_{cav}} \frac{\Delta\psi}{\pi}, \quad (1)$$

where  $c$  is the speed of light,  $\Delta\psi = \tan^{-1}(l_{cav}/2z_0) - \tan^{-1}(-l_{cav}/2z_0)$  is the Gouy phase shift of  $LG_{00}$ , and  $z_0$  the Rayleigh range of the cavity [9].

From this, we derive the expression for frequency spacing of  $LG_{00}$  and  $LG_{10}$  in terms of  $l_{cav}$  and  $R_C$ :

$$\Delta\nu_{trans} = \nu_{00} - \nu_{10} = \frac{c}{2l_{cav}} \left( 1 - \frac{\cos^{-1}g}{\pi} \right), \quad (2)$$

where  $g = 1 - l_{cav}/R_C$  the stability parameter.

To determine  $\Delta\nu_{trans}$  from the cavity transmission spectrum, we couple a frequency-stabilized 780 nm laser to the cavity and tune the  $l_{cav}$  within a free spectral range by applying a sawtooth voltage to the z-segment of the stacked piezo, which controls the cavity length. Fig 3 shows the cavity spectra when the cavity length is 600 nm and 210 nm shorter than the concentric point. We record the spectrum at multiple resonant cavity lengths and use a peak-detection algorithm to determine the resonance frequencies. Intensity distribution of cavity transmission on a linear camera helps us to distinguish different transverse modes. To obtain a frequency marker, we modulate the laser in phase by an electro-optical modulator (EOM). The two sidebands emerged as a result of the phase modulation of the laser are used as a frequency reference for the peak-detection algorithm.

Fig. 4 displays the transverse mode frequency spacing of cavity at different cavity lengths. From a least-squares fit of experimental data points to Eq. 2, we determine  $R_C = 5.49946(4)$  mm, which agrees well with the designed value. We would like to emphasize that the first data point in Fig. 4, which corresponds to the stability parameter  $g = -0.999996(28)$ , is the last geometrically

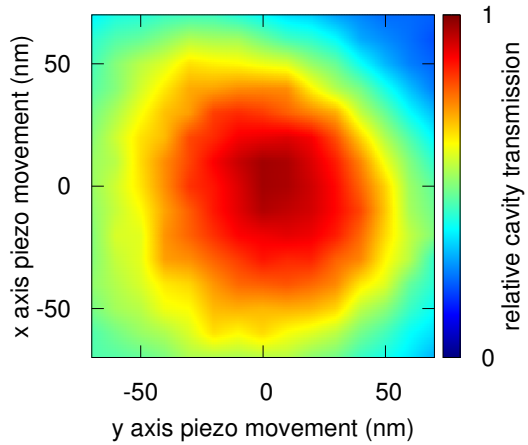


FIG. 5. Transversal profile of cavity transmission of the fundamental mode coupled to a single-mode fiber. The cavity length is maintained locked during the scanning.

stable point of the cavity that is resonant with 780 nm laser. By increasing the cavity length by another half wavelength, the cavity enters the unstable regime and exhibits lossy modes.

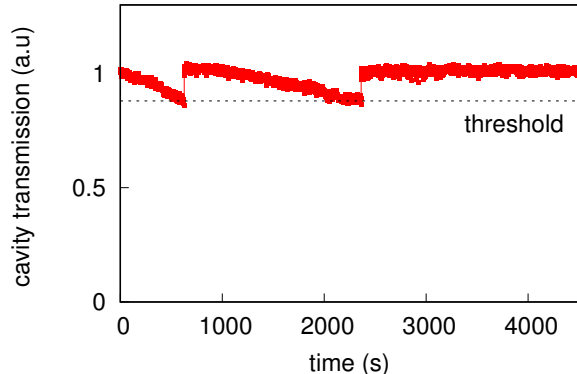


FIG. 6. Cavity transmission at  $l_{cav} = 2R - 210$ nm. The transversal compensation algorithm is activated when the cavity transmission drops below the threshold value which is chosen to be 10% of the maximum transmission. The cavity transmission recovers to the maximum value after the successful implementation of the algorithm.

#### IV. Stabilization of concentric cavities

In this section, we demonstrate the long-term stability of the cavity when operated at the last resonant length before concentric length and describe the algorithm to compensate for the drifting in transversal directions. Fig. 5 shows the 780 nm resonant transmission of the fundamental mode as we scan one of the cavity mirrors transversally. Throughout the experiment, the cavity length is locked to a frequency stabilized 810 nm laser via the standard Pound-Drever-Hall technique [10]. The

frequency of 810 nm laser is chosen such that the cavity is also resonant with 780 nm laser. The transmission profile in Fig. 5 shows a FWHM of 59(3) nm in transversal directions. Therefore, the change of temperature of the cavity on the order of 100mK is enough to reduce the transmission of the fundamental mode by 10%. To actively compensate for such drifting in alignment, we implement an algorithm based on gradient-search method to maximize the cavity transmission. The algorithm starts when the cavity transmission drops below a threshold value. The transversal positions of one cavity mirrors are scanned in incremental steps surrounding the initial location to find the direction of steepest descent of the cavity transmission. The algorithms repeat the iteration until the cavity transmission reach the chosen value within a predefined range of tolerance. The average search time when the cavity transmission drops by 10% is on the orders of seconds. Fig. 6 shows a typical record of cavity transmission at the last concentric point when the compensation algorithm is activated. The slow drift on the order of minutes is due to the temperature change of the cavity, while the

fast fluctuation of the maximum transmission is due to the vibration of the cavity length. With a combination of both temperature stabilization and active transversal compensation, the near-concentric cavity can stay on alignment for the course of few hours.

#### IV. Conclusion

To summarize, we present a compact design, alignment procedure and stabilization methods for a Fabry-Perot cavity that can be operated at sub-wavelength length shorter than the concentric point. The constructed cavity can be employed to explore multi-mode strong coupling CQED with various types of quantum emitters.

## ACKNOWLEDGMENTS

This work was supported by the Ministry of Education in Singapore (AcRF Tier 1) and the National Research Foundation, Prime Ministers office (partly under grant no NRF-CRP12-2013-03).

- 
- [1] A. Reiserer and G. Rempe, *Rev. Mod. Phys.* **87**, 1379 (2015).
  - [2] S. Ritter, C. Nolleke, C. Hahn, A. Reiserer, A. Neuzner, M. Uphoff, M. Mücke, E. Figueroa, J. Bochmann, and G. Rempe, *Nature* **484**, 195 (2012).
  - [3] A. Reiserer, N. Kalb, G. Rempe, and S. Ritter, *Nature* **508**, 237 (2014), arXiv:1404.2453.
  - [4] K. C. Cox, D. H. Meyer, N. A. Schine, F. K. Fatemi, and P. D. Kunz, (2018), arXiv:1802.05707.
  - [5] C. H. Nguyen, A. N. Utama, N. Lewty, K. Durak, G. Maslennikov, S. Straupe, M. Steiner, and C. Kurtsiefer, *Physical Review A* **96**, 031802 (2017), arXiv:1706.01256.
  - [6] H. Wang, M. Dovale-Álvarez, C. Collins, D. D. Brown, M. Wang, C. M. Mow-Lowry, S. Han, and A. Freise, *Physical Review D* **97**, 022001 (2018), arXiv:1711.05177.
  - [7] K. E. Ballantine, B. L. Lev, and J. Keeling, *Physical Review Letters* **118**, 045302 (2017).
  - [8] K. Durak, C. H. Nguyen, V. Leong, S. Straupe, and C. Kurtsiefer, *New Journal of Physics* **16**, 103002 (2014).
  - [9] B. E. A. Saleh and M. C. Teich, "Resonator Optics," in *Fundamentals of Photonics* (John Wiley & Sons, Inc., 2001) pp. 310–341.
  - [10] R. W. P. Drever, J. L. Hall, F. V. Kowalski, J. Hough, G. M. Ford, A. J. Munley, and H. Ward, *Applied Physics B* **31**, 97 (1983).